

Fermi-level effect on steady-state and transient photoconductivity in microcrystalline silicon

R. Brüggemann*

*Fachbereich Physik, Carl von Ossietzky Universität Oldenburg, D-26111 Oldenburg, Germany
and Institut für Physikalische Elektronik, Universität Stuttgart, Pfaffenwaldring 47, D-70569 Stuttgart, Germany*

C. Main

*School of Engineering, University of Abertay Dundee, Bell Street, Dundee DD1 1HG, Scotland, United Kingdom
(Received 3 March 1998)*

We show that steady-state and transient photoconductivity in microcrystalline silicon deposited by hot-wire chemical-vapor deposition depend strongly on the position of the Fermi level. The steady-state mobility-lifetime product increases significantly by shifting the Fermi level from around midgap towards the conduction or valence band. This increase corresponds to a slower decay in the transient photocurrent after pulsed excitation compared to the case with the Fermi level at midgap. We thus attribute the enhancement of the mobility-lifetime product to the increase of the lifetime of the majority carriers due to a change in the thermal occupation of defect centers by the shift in the Fermi level. The mobility-lifetime product information, often used as an indicator for material quality, should be complemented by the value of the dark conductivity, which monitors the Fermi level, in order to allow comparison between different samples. From our transient photo-response data we deduce a ratio of 10:1 for the mobility of electrons to the mobility of holes. [S0163-1829(98)50124-5]

I. INTRODUCTION

While nanometer grain-sized microcrystalline Si ($\mu\text{c-Si}$), which may thus also be called nanocrystalline Si (nc-Si), has been known for about 30 years,¹ the advent of very high-frequency (VHF) plasma-enhanced chemical-vapor deposition (PECVD) and catalytic or hot-wire assisted chemical vapor deposition (HW-CVD) has instigated new interest in this kind of semiconductor in order to understand and compare the electronic and optical properties as well as the structure and growth and the correlation between these. In HW-CVD,²⁻⁶ the catalytical decomposition of silane and hydrogen gas mixtures allows one to grow thin films on inexpensive substrates such as glass. A transition from microcrystalline to amorphous growth can be controlled by variation of the silane to hydrogen dilution.⁶ Doping by adding phosphine or diborane to the gas flow was achieved and varies the dark conductivity between $10^{-7} \Omega^{-1} \text{cm}^{-1}$ and $10^2 \Omega^{-1} \text{cm}^{-1}$.⁷ With the improvements in film quality, $\mu\text{c-Si}$ from HW-CVD has become a candidate for electronic and photovoltaic applications such as thin-film transistors and solar cells.^{8,9} Its prospects are thus similar to $\mu\text{c-Si}$ from VHF-PECVD.^{10,11} Both materials are being studied for the above-mentioned applications.¹²

We report a study of secondary steady-state photoconductivity (SSPC) and secondary transient photoconductivity (TPC) of HW-CVD $\mu\text{c-Si}$ in a series consisting of boron- and phosphorous doped, as well as undoped, samples in order to gain insight into the photoconductive properties, in particular, with respect to the position of the Fermi level in the band gap. The SSPC results were evaluated in terms of mobility-lifetime ($\mu\tau$) products, which reflect the properties of the majority carriers. In addition, TPC, which in our experiments means the study of the secondary transient photocurrent after pulsed excitation, provided additional informa-

tion based on the Fermi-level dependent decay kinetics that we correlate with the steady-state results. From our experiments we deduce that the commonly given $\mu\tau$ product as an indicator for the photoelectronic quality of the material should be complemented by the value of the dark conductivity as the value of the latter reflects the strong influence of the Fermi energy on the $\mu\tau$ product.

II. EXPERIMENT

The series of samples was deposited at the Institut für Physikalische Elektronik, Universität Stuttgart, by HW-CVD at 400 °C with a growth rate of 10 Å/s and typical thicknesses around 1 μm . The hydrogen dilution ratio, defined as the sum of silane plus doping gas flow rate to hydrogen gas flow rate, was fixed to 1:30. More details on the deposition parameters and the crystallinity of the samples monitored by ellipsometry and Raman experiments are given in Refs. 7, 8, and 12. Coplanar Al electrodes were deposited for the secondary photoconductivity measurements.

A HeNe laser at 632.8 nm provided the monochromatic steady state illumination conditions. The $\mu\tau$ products were calculated from $\sigma_{\text{ph}}/(eG)$ where σ_{ph} is the photoconductivity, e is the elementary charge, and G the photogeneration rate for which we assumed a quantum efficiency η of unity.

We recorded transient photocurrents after pulsed excitation with a N-pumped dye laser with 4 ns pulse width at a wavelength of 640 nm. The experimental setup for sampling the photocurrent decay from about 10 ns over many orders of magnitude in both time and current is the same as described in Refs. 13 and 14. For comparison, we normalize the currents with the factor eN_0EA ,¹⁵ where N_0 is the initial excess carrier density, determined with a fast photodiode and $\eta = 1$, E the electric field and A the conduction cross section, in order to represent the physical properties for the different

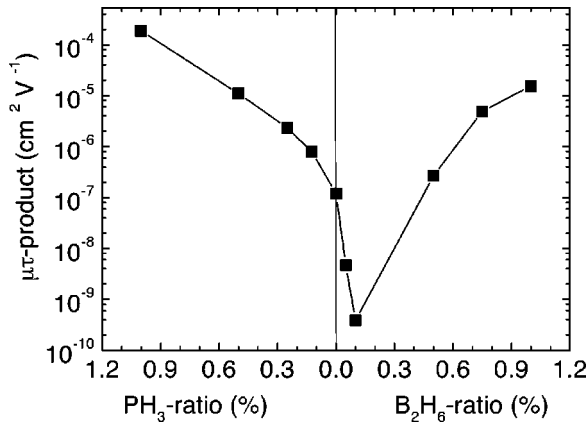


FIG. 1. Steady-state $\mu\tau$ products for B and P doping. The abscissa defines the doping gas PH_3 ratio and B_2H_6 ratio as $[\text{PH}_3]/([\text{PH}_3] + [\text{SiH}_4])$ (%) and $[\text{B}_2\text{H}_6]/([\text{B}_2\text{H}_6] + [\text{SiH}_4])$ (%), which is used in the other figures as a parameter for identifying the samples.

Fermi levels independent of the particular sample geometry and applied voltage (which had to be varied due to the large differences in the dark conductivity σ_D). The scaling is the same as employed for TPC in amorphous semiconductors and results in a transient drift mobility $\mu_d(t)$ ^{14,15} that describes the transport when there is only a fraction of excess carriers in the band.

III. RESULTS

Figure 1 shows the $\mu\tau$ products of the sample series for a photon flux $\Phi = 1.4 \times 10^{18} \text{ cm}^{-2} \text{ s}^{-1}$, exhibiting a strong increase in magnitude for the higher doping ratios for both B and P doping together with a deep minimum for slight B doping. These values for the $\mu\tau$ products are intimately linked to measured σ_D , i.e., the sample with the lowest σ_D has the lowest $\mu\tau$ product and the increase in $\mu\tau$ scales with the increase in σ_D .¹⁶

Figure 2 displays the TPC decays of three samples of the series with different doping and with significant differences in $\mu\tau$. The dark conductivity is $7 \times 10^{-2} \text{ } \Omega^{-1} \text{ cm}^{-1}$ for the P-doped sample and $1.7 \times 10^{-6} \text{ } \Omega^{-1} \text{ cm}^{-1}$ (1.4×10^{-2}

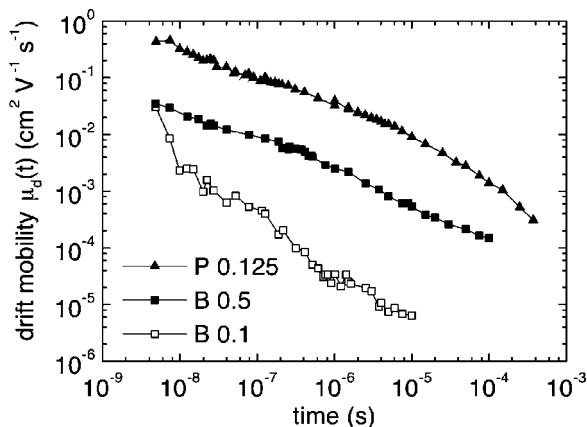


FIG. 2. Normalized TPC decays for three differently doped samples from Fig. 1. The legend gives the doping gas ratio, defined in Fig. 1, together with the type of doping.

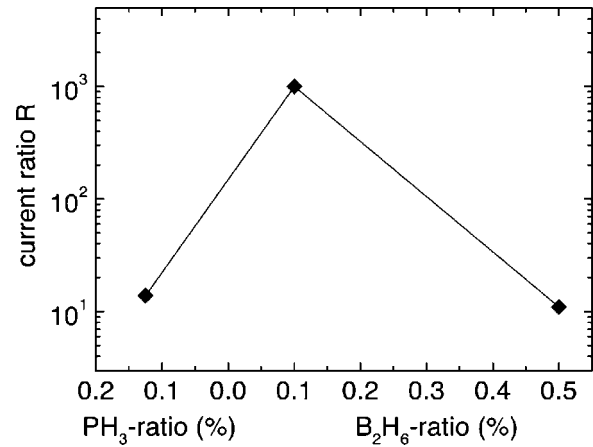


FIG. 3. Photocurrent decay rate ratio $R = I_{\text{ph}}(5 \text{ ns})/I_{\text{ph}}(1 \text{ } \mu\text{s})$ for the different doping gas ratios matches inversely with the shape of the steady-state results in Fig. 1.

$\Omega^{-1} \text{ cm}^{-1}$) for a gas flow ratio of 0.1% (0.5%) for the two B-doped samples. The decay curve in Fig. 2 for the lowest B-doping level shows a steep decay whereas the samples with larger $\mu\tau$ and σ_D exhibit a slower decay independent of whether the majority carriers are expected to be electrons (holes) for n -type (p -type) doping. The magnitude of the currents, which also differs for the samples, reflects the proportion of excess carriers that are free and contribute to the current.

The TPC decays are nonexponential so that in order to display a measure of the rates of the decay we calculate the ratio R of the transient photocurrent I_{ph} , defined by $R = I_{\text{ph}}(5 \text{ ns})/I_{\text{ph}}(1 \text{ } \mu\text{s})$. As shown in Fig. 3, the samples from Fig. 2 with higher doping have a smaller and about equal value for R , i.e., a smaller decay rate, compared to the lightly B-doped sample.

IV. DISCUSSION

The large increase in the steady-state $\mu\tau$ products upon higher doping is related to the shift of the Fermi level towards the valence (conduction) band for p -type (n -type) doping. That a Fermi-level shift does take place with doping is reflected by the large increase in the dark conductivity upon addition of B and P, and also by the observed decrease in the dark conductivity activation energy. The thermal occupation of any distribution of recombination centers in the band gap will thus change when the Fermi level shifts and the density of centers that capture majority carriers is greatly reduced by the change in thermal occupation. For example, if the Fermi level is close to the conduction band most defects will be thermally occupied by electrons and inaccessible for excess electrons, thus leading to a large electron lifetime and the large $\mu\tau$ product in Fig. 1. On the other hand, a Fermi-level position around the middle of the band gap makes more centers available for electron capture. Similar arguments hold for shifting the Fermi level towards the valence band.

We support this interpretation by our TPC results in Fig. 2. The transient photocurrent response is determined by capture into the recombination centers but also, for example, in amorphous semiconductors, by the capture and reemission from shallower states leading to the typical nonexponential

decay in these semiconductors.¹⁷ Our material consists of nanometer-size crystallites with grain sizes between 6 and 10 nm that are embedded into larger columnar structures with negligible overall amorphous fraction.⁸ For the lowest $\mu\tau$ product with the very small value of a few times $10^{-10} \text{ cm}^2 \text{ V}^{-1}$ in Fig. 1, the typical drift length $L_d = E\mu\tau$ is below 10 nm, depending on the typical experimental field E of 500 to $2 \times 10^3 \text{ V/cm}$. For this low $\mu\tau$ product the drift length is smaller than the size of the crystallites. In the samples with the larger $\mu\tau$ products any charge carrier passes many crystallites before eventual recombination. In our $\mu\text{c-Si}$ the recombination centers may be located at the boundaries of the columnar structures as suggested from spin-resonance experiments,¹⁸ but more work is needed for a clear identification.

In our qualitative account we cannot expect that the TPC-decay rates or decay times match the steady-state $\mu\tau$ variation exactly. The shape of the TPC-decay rate variation in Fig. 3, which follows the shape of the $\mu\tau$ data for the different doping levels intriguingly closely, is encouraging for our interpretation. The decay for the lightly doped sample is thus fastest because the low steady-state $\mu\tau$ product can be translated into a large density of available deeper states. In contrast, for higher doping and larger σ_D where the Fermi level shifted from midgap, the decay rates, as given by the largest values of the photocurrent ratio R , are smallest as most defects are already thermally occupied. The situation is similar to the photoresponse of hydrogenated amorphous silicon. The majority carrier $\mu\tau$ in this semiconductor also increases upon doping¹⁹ in combination with a slower decay after pulsed excitation.²⁰

We note that the rate of decay for the two samples with higher doping is the same but their absolute values of the normalized currents or transient drift mobilities in Fig. 2 are different. We attribute this to the difference in mobility of the majority carriers, suggesting a ten times higher mobility for the electrons in the n -type sample as compared to the holes in the p -type sample.

Noting that the normalized currents are scaled to transient drift mobilities $\mu_d(t)$ we find values around $10^{-1} \text{ cm}^2 \text{ V}^{-1} \text{ s}^{-1}$ at about 1 ns. This value takes into account interaction with traps leading to multiple-trapping transport. Performing the transient photoconductivity experiment in sandwich configuration for primary photocurrents as in time-of-flight and thus with transport in parallel to the growth direction will allow a direct comparison for studying any anisotropy of transport in this semiconductor.

Two other factors will also influence the change in the photoelectronic properties with doping as discussed above. A change in mobility and a change in the density of defects may occur upon doping with either B or P. The different TPC-decay behavior clearly indicates that the lifetime is the most important factor for the increase in $\mu\tau$. Available Hall mobility data, from the B-doped samples only, show values around $3 \text{ cm}^2 \text{ V}^{-1} \text{ s}^{-1}$ with no systematic increase upon doping.²¹ From the related VHF-PECVD $\mu\text{c-Si}$, Backhausen *et al.*²² show Hall mobility changes of only less than a factor of 3 for different doping levels. Carius *et al.* report that the Hall mobility changes with grain size in VHF-PECVD

material.²³ Although we deal with HW-CVD $\mu\text{c-Si}$ here we note that the grain size for the differently doped samples studied varies only between 6 nm and 10 nm,^{21,16} supporting the view that it is the lifetime change that leads to the increase in $\mu\tau$ with higher doping.

Any possible increase in the density of defects upon doping, which again we cannot rule out, is effectively counterbalanced by the reduction of the effective density of defects that become unavailable for majority-carrier capture through their thermal occupation. Additional experiments for a doping series like electron-spin resonance (ESR) and a deconvolution of the spectra recorded by the constant photocurrent method (CPM) will help to further consolidate the understanding about the nature and location of the defects in hot-wire $\mu\text{c-Si}$.

There are two more conclusions to be drawn. The fact that HW-CVD $\mu\text{c-Si}$ can be efficiently doped indicates a density of localized states low enough for the Fermi level to shift across the distribution, i.e., the Fermi level is not pinned, leading to the large majority-carrier lifetime. From the TPC results we deduce that there are localized states in the band gap with which the free carriers interact. These are large enough in density so as to reduce the drift mobility to the values observed. The nature of the states needs to be further clarified, for which the experimental methods applied here in combination with the above-mentioned ESR or CPM are important means.

V. CONCLUSIONS

Our results reveal a large increase in the steady-state $\mu\tau$ product and in the lifetime of the majority carriers in our related experiments of steady-state and transient photoconductivity in hot-wire deposited $\mu\text{c-Si}$. We attribute these increased values for both B and P doping to the change in thermal occupation of the recombination centers induced by the Fermi-level shift. From the similar rates of decay for the majority electrons and holes for the more highly doped samples we deduce an approximately ten times larger mobility for electrons than for holes. In view of the observed variation, we suggest that the $\mu\tau$ product be complemented by values for the dark conductivity or Fermi level if given as an indicator for material quality, noting that undoped $\mu\text{c-Si}$ samples also show different dark conductivity values.

We expect the steady-state and transient photoconductivity to become strong tools for revealing more about the nature of defects in $\mu\text{c-Si}$ and the related problems of recombination, especially when they are to be complemented by additional experimental techniques like electron-spin resonance.

ACKNOWLEDGMENTS

The authors acknowledge funding from the DAAD and British Council via the ARC collaboration, and thank H. N. Wanka for providing the samples, I. Zrinščak for standard sample characterization, and S. Reynolds for experimental assistance. A critical reading of the manuscript by U. Rau is gratefully acknowledged.

- *Electronic address: rudi@greco6.physik.uni-oldenburg.de
- ¹S. Vepřek and V. Mareček, *Solid-State Electron.* **11**, 683 (1968).
- ²H. Wiesmann, A. K. Ghosh, T. McMahon, and M. Strongin, *J. Appl. Phys.* **50**, 3752 (1979).
- ³H. Matsumura, *Jpn. J. Appl. Phys., Part 2* **25**, L949 (1986).
- ⁴J. Cifre, J. Bertomeu, J. Puigdollers, M. C. Polo, J. Andreu, and A. Lioret, *Appl. Phys. A: Solids Surf.* **59**, 645 (1994).
- ⁵A. R. Middy, J. Guillet, J. Perrin, A. Lloret, and J. E. Bourree, in *Proceedings of the 13th European Photovoltaic Solar Energy Conference, Nice, 1995*, edited by W. Freiesleben, W. Palz, H. A. Ossenbrink, and P. Helm (H.S. Stephens & Associates, Bedford, U.K., 1995), p. 3.
- ⁶M. Heintze, R. Zedlitz, H. N. Wanka, and M. B. Schubert, *J. Appl. Phys.* **79**, 2699 (1996).
- ⁷H. Wanka, R. Zedlitz, M. Heintze, and M. B. Schubert, in *Proceedings of the 13th European Photovoltaic Solar Energy Conference, Nice, 1995* (Ref. 5), p. 1753.
- ⁸H. Wanka, M. B. Schubert, A. Hierzenberger, and V. Baumung, in *Proceedings of the 14th European Photovoltaic Solar Energy Conference, Barcelona, 1997*, edited by H. A. Ossenbrink, P. Helm, and H. Ehmann (H.S. Stephens & Associates, Bedford, U.K., 1997), p. 1003.
- ⁹R. E. I. Schropp, K. F. Feenstra, E. C. Molenbroek, H. Meiling, and J. K. Rath, *Philos. Mag. B* **76**, 309 (1997).
- ¹⁰J. Meier, S. Dubail, R. Flückinger, D. Fischer, H. Keppner, and A. Shah, in *Conference Record 24th IEEE Photovoltaic Specialists Conference, Hawaii, 1994*, edited by Editors (IEEE, New York, 1994), p. 409.
- ¹¹D. Fischer, S. Dubail, J. A. Anna Selvan, N. Pellaton Vaucher, R. Platz, C. Hof, U. Kroll, J. Meier, P. Torres, H. Keppner, N. Wyrsh, M. Goetz, A. Shah, and K.-D. Ufert, in *Conference Record 25th IEEE Photovoltaic Specialists Conference, Washington, D.C., 1996*, edited by Editors (IEEE, New York, 1996), p. 1053.
- ¹²H. Brummack, R. Brüggemann, H. N. Wanka, A. Hierzenberger, and M. B. Schubert, in *Conference Record 26th IEEE Photovoltaic Specialists Conference, Anaheim, 1997*, edited by Editors (IEEE, New York, 1998).
- ¹³C. Main, R. Brüggemann, D. P. Webb, and S. Reynolds, *J. Non-Cryst. Solids* **164-166**, 481 (1993).
- ¹⁴R. Brüggemann, C. Main, M. Rösch, and D. P. Webb, in *Amorphous Silicon Technology-1996*, edited by M. Hack *et al.*, MRS Symposia Proceedings No. 420 (Materials Research Society, Pittsburgh, 1996), p. 697.
- ¹⁵H. Antoniadis and E. A. Schiff, *Phys. Rev. B* **44**, 3627 (1991).
- ¹⁶R. Brüggemann, A. Hierzenberger, P. Reinig, M. Rojahn, M. B. Schubert, S. Schweizer, H. N. Wanka, and I. Zrinščak, *J. Non-Cryst. Solids* **227-230**, 982 (1998).
- ¹⁷J. M. Marshall, *Rep. Prog. Phys.* **46**, 1235 (1983).
- ¹⁸K. Lips, P. Kanschä, and W. Fuhs, *J. Non-Cryst. Solids* **227-230**, 1021 (1998).
- ¹⁹J. Kočka, C. E. Nebel, and C.-D. Abel, *Philos. Mag. B* **63**, 221 (1991).
- ²⁰C. Main, R. Russell, J. Berkin, and J. M. Marshall, *Philos. Mag. Lett.* **55**, 189 (1987).
- ²¹H. N. Wanka (private communication).
- ²²U. Backhausen, R. Carius, F. Finger, P. Hapke, U. Zastrow, and H. Wagner, in *Advances in Microcrystalline and Nanocrystalline Semiconductors-1996*, edited by R. W. Collins *et al.*, MRS Symposia Proceedings No. 452 (Materials Research Society, Pittsburgh, 1997), p. 633.
- ²³R. Carius, F. Finger, M. Luysberg, P. Hapke, and U. Backhausen, in *Future Directions in Thin Film Science and Technology*, edited by J. M. Marshall *et al.* (World Scientific, Singapore, 1997), p. 11.